GSVD-Based Uplink Channel Diagonalization in OTFS for Multi-User Systems*

Omid Abbassi Aghda[1,2,*,†], Oussama Ben Haj Belkacem[1,3,†], João Guerreiro[1,2,†], Nuno Souto[1,4,†], Michal Szczachor[5,†] and Rui Dinis[1,2,†]

[1]Instituto de Telecomunicações, Lisboa, Portugal
[2]Universidade Nova de Lisboa, Monte da Caparica, 2829-516 Caparica, Portugal
[3]Innov'Com Laboratory, Sup'Com, University of Carthage, Tunis 1054, Tunisia
[4]ISCTE-Instituto Universitário de Lisboa, 1649-026 Lisbon, Portugal
[5]Nokia, Wroclaw, Poland

Abstract

This paper introduces a multi-user uplink system, utilizing the orthogonal time frequency space (OTFS) modulation scheme. The proposed design employs the generalized singular value decomposition (GSVD) of the channels connecting the base station and the two users. Precoding and detection matrices are constructed using the right and left singular vectors, respectively. Analytical expressions are derived for a practical antenna configuration, and corresponding simulation results are presented. Simulation results for uncoded, coded, and coded scenarios with channel estimation errors reveal that the proposed GSVD-based approach outperforms MMSE equalization in certain antenna configurations. Notably, GSVD shows advantages under channel estimation error in the coded scenario.

Keywords

OTFS, GSVD, MIMO, Multi-User, System Design, Performance Evaluation

1. INTRODUCTION

Ensuring reliable communication for high-speed users is a key requirement in sixth-generation (6G) wireless networks. OTFS modulation, tailored for such environments, operates in the delay-Doppler domain, enabling it to handle the effects of both delay and Doppler spread in the channel [1, 2]. However, multiple access techniques for OTFS modulation are still under development and require further research [3].

Various studies have explored orthogonal multiple access (OMA) techniques in orthogonal time frequency space (OTFS) modulation; however, these methods are not based on precoding approaches and do not employ the spatial multiplexing capabilities of MIMO systems for transmission. In [4], the authors proposed a multiplexing method in the delay-Doppler (DD) domain, where different DD bins are allocated to separate users. While this approach is straightforward at the transmitter side, each user is required to mitigate interference from others at the receiver. To address this challenge, guard intervals can be introduced between the multiplexed data in the DD domain, though this comes at the cost of reduced spectral efficiency. In [5], resource allocation in the time-frequency (TF) domain was proposed for OTFS modulation, with information symbols being interleaved in the DD domain to ensure contiguity in the TF domain. In [6], an uplink multiple access (MA) scheme was introduced based on Orthogonal Frequency Division Multiplexing (OFDM) modulation for single input single output (SISO) systems, demonstrating that the concatenated signals from all users at the base station (BS) behave equivalently to a single-user OTFS system. This work was later extended in [7], where the authors investigated the uplink scenario for multiple-input multiple-output (MIMO) systems.

WIPHAL'25: Work-in-Progress in Hardware and Software for Location Computation June 10–12, 2025, Rome, Italy
*Corresponding author.
These authors contributed equally.
o.aghda@campus.fct.unl.pt (O. A. Aghda); belkacemoussema@yahoo.fr (O. B. H. Belkacem); jf.guerreiro@fct.unl.pt (J. Guerreiro); nuno.Souto@iscte-iul.pt (N. Souto); michal.szczachor@nokia.com (M. Szczachor); rdinis@fct.unl.pt (R. Dinis)

In contrast to methods that do not utilize precoding or spatial multiplexing, several studies have investigated precoding schemes for OTFS systems to enhance performance. In [8], the authors evaluated two cases for downlink precoding. In the first case, they considered ideal pulse shaping, leveraging bi-orthogonality to diagonalize the doubly selective channel matrix. The second case focused on practical pulse shaping, where precoders were designed in the TF domain and subsequently transformed into the DD domain for implementation. In [9], a downlink precoding approach leveraging Tomlinson-Harashima precoding was introduced, utilizing the interference pattern in the DD domain for enhanced performance. In [10], the authors proposed a joint precoding and equalization scheme for the uplink multi-user case, aimed at reducing computational complexity and minimizing CSI feedback overhead through the use of statistical Doppler shift information and optimized matrix dimensions. In [11], the authors proposed a precoding scheme for a MIMO system focused on a single-user scenario to maximize the achievable rate of MIMO-OTFS in the presence of beam squint, leaving room for potential exploration in multi-user systems.

In the context of OTFS modulation, non-orthogonal multiple access (NOMA) has also been investigated. For instance, a deep learning-based approach for signal detection in a two-user downlink SISO-NOMA system was introduced in [12]. Similarly, [13] presented a robust beamforming technique for a two-user downlink MIMO system. This strategy allocates the low mobility user's data within the TF domain and guarantees that the high mobility user's requirements are met by placing its data in the DD domain. Furthermore, the work in [14] proposed the use of an interference alignment (IA) matrix as a precoder to mitigate inter-user interference (IUI) in a multi user (MU) MIMO-OTFS downlink scenario. They also explored data detection using singular value decomposition (SVD) combined with precoding to simplify the channel matrix.

Although extensive research has been conducted, equalization remains a significant challenge in OTFS modulation. The transceiver's input-output relationship in the DD domain is characterized by a 2 dimensional (2D) phase-rotated convolution between the transmitted signal and the channel impulse response in this domain [2]. This 2D convolution introduces complexities that make OTFS channel equalization and data detection computationally intensive, in contrast to OFDM, which supports a straightforward single-tap equalizer. In high-speed environments, frequency domain equalization (FDE) proves inadequate for OTFS, unlike its effectiveness in low-mobility scenarios with single carrier modulation (SCM), where a single-tap equalizer is feasible. However, it is crucial to note that while detection in OTFS can be complex, the system's performance remains robust across varying user speeds, provided a suitable equalization or detection method is employed. This contrasts with high mobility systems using OFDM and SCM.

The concept of generalized singular value decomposition (GSVD) decomposition was first presented in [15] and later expanded with a more detailed definition in [16]. To extend this method to multiple matrices, the Higher Order GSVD (HO-GSVD) was introduced in [17]. Furthermore, [18] explored the application of GSVD in wireless communication, employing it to divide a wireless channel for two users into the private channel (PC) and common channel (CC), and providing an exhaustive description of both interpretations of GSVD.

Our contribution in this paper is the development of a precoding and detection scheme for a MU MIMO-OTFS system based on GSVD decomposition. This decomposition allows us to reduce the channel matrix to a diagonal form, thereby avoiding the need to handle a 2D circular convolution at the receiver. We then evaluate the performance of the proposed system and compare it with minimum mean square error (MMSE) equalization. Our proposed method demonstrates superiority over the mentioned methods.

Notation: In the remainder of this paper, boldface uppercase letters represent matrices, boldface lowercase letters denote vectors, and standard lowercase letters correspond to scalars. The symbols $(.)^H$, $(.)^T$, and vec$(.)$ are used to signify Hermitian, transpose, and column-wise vectorization operations, respectively. Additionally, $\mathbf{A}_{\{:,1:k\}}$ denotes the selection of the first to the k^{th} columns of the matrix $\mathbf{A}$. The terms $\mathbf{I}$ and $\mathbf{0}$ refer to the identity matrix and the zero matrix, respectively.

2. OTFS SYSTEM MODEL

Consider a DD grid of size $M \times N$ representing a discrete delay-Doppler (DD) domain. The delay axis is divided into M bins indexed by $l = 0, 1, \ldots, M-1$, where each bin corresponds to a delay of $\tau = \frac{1}{B}$ seconds, while the Doppler axis is divided into N bins indexed by $k = 0, 1, \ldots, N-1$, where each bin corresponds to a Doppler shift of $\nu = \frac{1}{T_f}$ Hz. Here, B denotes the available bandwidth, and T_f represents the frame length. Consequently, the corresponding sub-carrier spacing and subsymbol duration in the time-frequency (TF) domain are given by $\Delta f = \frac{B}{M}$ and $T_s = \frac{T_f}{N}$, respectively. The relationship between the DD domain and the TF domain is established through the symplectic finite Fourier transform (SFFT) [19].

2.1. UPLINK SYSTEM MODEL

Consider an uplink system with two users, each equipped with G_u antennas ($u = 0, 1$), and a base station equipped with C antennas.[1] A DD domain grid is employed for each antenna at the transmitter of each user to represent precoded information symbols. The transmitted precoded signal at the g^{th} antenna of the u^{th} user in the DD domain is denoted by $\mathbf{X}_{u,g}$. The received signal at the c^{th} antenna of the base station is

$$\mathbf{y}_c = \sum_{u=1}^{U} \sum_{g=1}^{G_u} \mathbf{H}_{c,u,g} \mathbf{x}_{u,g} + \mathbf{n}_c \tag{1}$$

where $\mathbf{y}_c \in \mathbb{C}^{MN \times 1}$ for $c = 1, \ldots, C-1$ and $U = 2$. The matrix $\mathbf{H}_{c,u,g} \in \mathbb{C}^{MN \times MN}$ represents the channel matrix between the g^{th} antenna of user u and the c^{th} antenna of the base station.[2] For the remainder of this paper, it is assumed that the channel matrices $\mathbf{H}_{c,u,g}$ are full rank, indicating that the physical environment is rich in terms of the number of multipath components. The vector $\mathbf{x}_{u,g} \in \mathbb{C}^{MN \times 1}$ is the vectorized form of the matrix $\mathbf{X}_{u,g}^T$. The vector $\mathbf{n}_c$ represents the additive white Gaussian noise (AWGN) where its elements are independently distributed $\mathbf{n}_c(.) \sim \mathcal{N}(0, \sigma^2)$.

By considering all antennas together, the input-output relationship of the overall system can be written as

$$\mathbf{y} = \sum_{u=1}^{U} \mathbf{H}_u \mathbf{x}_u + \mathbf{n} \tag{2}$$

where

$$\mathbf{H}_u = \begin{bmatrix} \mathbf{H}_{1,u,1} & \mathbf{H}_{1,u,2} & \cdots & \mathbf{H}_{1,u,G_u} \\ \mathbf{H}_{2,u,1} & \mathbf{H}_{2,u,2} & \cdots & \mathbf{H}_{2,u,G_u} \\ \vdots & \ddots & \ddots & \vdots \\ \mathbf{H}_{C,u,1} & \mathbf{H}_{C,u,2} & \cdots & \mathbf{H}_{C,u,G_u} \end{bmatrix} \in \mathbb{C}^{MNC \times MNG_u} \tag{3}$$

is the channel matrix between the u^{th} user and the receiver. The vectors $\mathbf{x}_u \in \mathbb{C}^{MNG_u \times 1}$, $\mathbf{y} \in \mathbb{C}^{MNC \times 1}$, and $\mathbf{n} \in \mathbb{C}^{MNC \times 1}$ represent the transmitted vector of the u^{th} user, the received vector, and the noise vector from all antennas of the receiver, respectively. These vectors are given by

$$\mathbf{x}_u = \begin{bmatrix} \mathbf{x}_{u,1} \\ \mathbf{x}_{u,2} \\ \vdots \\ \mathbf{x}_{u,G_u} \end{bmatrix}, \quad \mathbf{y} = \begin{bmatrix} \mathbf{y}_1 \\ \mathbf{y}_2 \\ \vdots \\ \mathbf{y}_C \end{bmatrix}, \quad \mathbf{n} = \begin{bmatrix} \mathbf{n}_1 \\ \mathbf{n}_2 \\ \vdots \\ \mathbf{n}_C \end{bmatrix}. \tag{4}$$

[1] This work can be extended to support multiple users by applying HO-GSVD [17].

[2] The structure of the matrix $\mathbf{H}_{c,u,g}$ is fully explained in [19, Chapter 4].

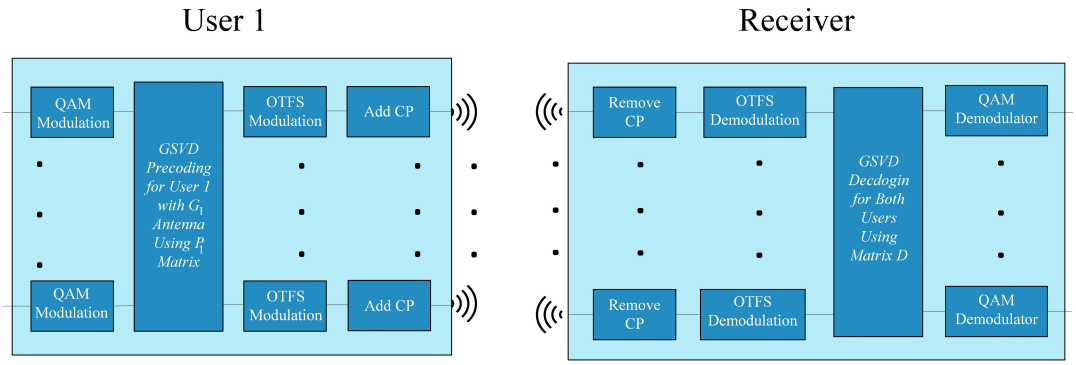

Figure 1: Block diagram of an uplink system for User 1; User 2 follows the same structure.

3. GSVD DECOMPOSITION, RECODING AND DETECTION MATRIX

We define the following parameters as $k_u = \text{rank}\,(\mathbf{H}_u)$, and $k = \text{rank}\left(\begin{bmatrix}\mathbf{H}_1 & \mathbf{H}_2\end{bmatrix}\right)$. Based on the GSVD, the channel matrices $\mathbf{H}_u^H$ are decomposed as:

$$\mathbf{H}_u^H = \mathbf{U}_u \mathbf{\Sigma}_u \begin{bmatrix}\mathbf{W}^H\mathbf{R} & \mathbf{0}\end{bmatrix} \mathbf{Q}^H = \mathbf{U}_u \mathbf{\Sigma}_u \mathbf{V}^H. \tag{5}$$

Here:

- $\mathbf{U}_u \in \mathbb{C}^{MNG_u \times MNG_u}$ are unitary matrices
- $\mathbf{\Sigma}_u \in \mathbb{C}^{MNG_u \times MNk}$ are block diagonal matrices
- $\mathbf{W} \in \mathbb{C}^{k\times k}$, $\mathbf{Q} \in \mathbb{C}^{MNC\times MNC}$ are unitary matrices
- $\mathbf{R} \in \mathbb{C}^{k\times k}$ is an invertible matrix
- $\mathbf{0} \in \mathbb{R}^{k\times(MNC-k)}$
- $\mathbf{V}^H \in \mathbb{C}^{k\times MNC}$

In this case, and with the assumption that the channel matrices are full rank, the matrices $\mathbf{\Sigma}_1$ and $\mathbf{\Sigma}_2$ can be expressed as block diagonal matrices with the following specifications:

$$\mathbf{\Sigma}_1 = \begin{bmatrix}\mathbf{I}_1 & & \\ & \mathbf{S}_1 & \\ & & \mathbf{0}_1\end{bmatrix}, \mathbf{\Sigma}_2 = \begin{bmatrix}\mathbf{0}_2 & & \\ & \mathbf{S}_2 & \\ & & \mathbf{I}_2\end{bmatrix} \tag{6}$$

where:

- $\mathbf{I}_1 \in \mathbb{R}^{(k-k_2)\times(k-k_2)}$, $\mathbf{I}_2 \in \mathbb{R}^{(k-k_1)\times(k-k_1)}$
- $\mathbf{0}_1 \in \mathbb{R}^{(MNG_1-k_1)\times(k-k_1)}$,$\mathbf{0}_2 \in \mathbb{R}^{(MNG_2-k_2)\times(k-k_2)}$
- $\mathbf{S}_u = \text{diag}\,(\sigma_{1,u}, \sigma_{2,u}, \ldots, \sigma_{k_1+k_2-k,u}) \in \mathbb{C}^{(k_1+k_2-k)\times(k_1+k_2-k)}$ are diagonal matrices containing the channel gains, where $\sqrt{\sigma_{i,1}^2 + \sigma_{i,2}^2} = 1$ for $i = 1, \ldots, k_1 + k_2 - k$

Based on the GSVD in (5), the precoding and detection matrices are respectively defined as[3]

$$\mathbf{P}_u = \mathbf{U}_u, \quad \mathbf{D} = \mathbf{W}\mathbf{R}^{-1}(\mathbf{Q}_{\{:,1:k\}})^H \in \mathbb{C}^{k\times MNC} \tag{7}$$

Considering G_u data streams for each user, the precoded vector in the transmitter of each user is

$$\mathbf{x}_u = \mathbf{P}_u \mathbf{s}_u \tag{8}$$

where the vector $\mathbf{s}_u \in \mathbb{C}^{MNG_u\times 1}$ contains the information quadrature amplitude modulation (QAM) symbols for each user.

[3]In simulation, we used the equivalent detection matrix considering the noise reduction as $\mathbf{D} = (\mathbf{V}^H\mathbf{V} + \sigma^2\mathbf{I})^{-1}\mathbf{V}^\mathbf{H}$

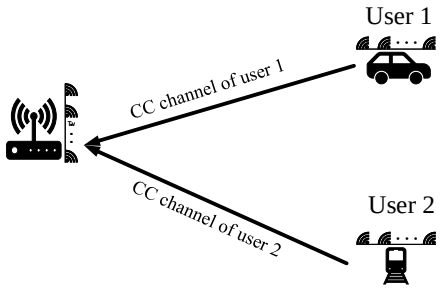

Figure 2: Transmission scheme while $G_1 + G_2 < C$

Fig. 1 depicts the block diagram of the system's transmitter and receiver. In the receiver, the detection matrix is applied to the received signal $\mathbf{y}$ in (2), resulting in

$$\mathbf{r} = \mathbf{D}\mathbf{y} = \mathbf{D}\mathbf{H}_1\mathbf{x}_1 + \mathbf{D}\mathbf{H}_2\mathbf{x}_2 + \mathbf{D}\mathbf{n} \tag{9}$$

By substituting (5), (7), and (8) into (9), the following is obtained

$$\mathbf{r} = \mathbf{\Sigma}_1^H\mathbf{s}_1 + \mathbf{\Sigma}_2^H\mathbf{s}_2 + \mathbf{D}\mathbf{n} \tag{10}$$

In (10), the term $\mathbf{D}\mathbf{n}$ leads to noise enhancement since the matrix $\mathbf{D}$ is not unitary. However, in (7), the precoding matrix $\mathbf{U}_u$ is unitary.

In this paper, we consider a realistic scenario where $G_1 + G_2 \leq C$. Given that the matrix $\mathbf{H}$ has full rank and $G_1 + G_2 < C$, the matrices $\mathbf{\Sigma}_1^H$ and $\mathbf{\Sigma}_2^H$ reduce to the following forms because, in this case, $k = MN(G_1 + G_2)$, $k_1 = MNG_1$, and $k_2 = MNG_2$:

$$\mathbf{\Sigma}_1^H = \begin{bmatrix} \mathbf{I}_1 \\ \mathbf{0}_{(k-k_1)\times(k-k_2)} \end{bmatrix}, \mathbf{\Sigma}_2^H = \begin{bmatrix} \mathbf{0}_{(k-k_2)\times(k-k_1)} \\ \mathbf{I}_2 \end{bmatrix} \tag{11}$$

Comparing (11) and (10) yields

$$\mathbf{r} = \begin{bmatrix} \mathbf{s}_1 \\ \mathbf{s}_2 \end{bmatrix} + \mathbf{D}\mathbf{n} \tag{12}$$

Now, the information from each user can be easily extracted in the presence of noise. Fig. 2 illustrates the uplink setup and user configuration in a high-speed environment.

4. SIMULATION RESULTS

This section focuses on evaluating the performance of the proposed GSVD approach. The simulation setup parameters are detailed in Table 1. The channel model considered is the Extended Vehicular A (EVA) channel, as defined in the 3rd Generation Partnership Project (3gpp) TS 36.104 [20]. The maximum environmental speed is set to $v_{\max} = 500$ km/h, resulting in a maximum Doppler frequency shift and normalized Doppler shift of $\nu_{\max} = \frac{v_{\max} \times f_c}{\text{light speed}} = 1853$ Hz and $k_{\max} = \nu_{\max} T_f = 0.9883$, respectively. The modulation scheme employed is 4-QAM, which maps the information bits into corresponding symbols. We compared the performance of our proposed GSVD method with MMSE equalization in terms of bit error rate (BER), using two MU-MIMO antenna configurations: $(3+2) \times 6$ and $(1+1) \times 6$. The evaluation was conducted across three scenarios: one without channel coding, one using a 3/4 low-density parity check (LDPC) code as specified in the IEEE 802.11 standard with a block length of 648, and another incorporating channel coding while accounting for channel estimation errors.

Fig. 3 illustrates the BER curve as a function of signal-to-noise ratio (SNR). For the $(1+1) \times 6$ configuration, the simulation results show a slight gap between the GSVD and MMSE methods, with MMSE exhibiting marginally better performance. Notably, both users achieve identical performance.

Table 1
Simulation parameters

Parameters	Values
Carrier frequency	$f_c = 4$ GHz
Sub-carrier spacing	$\Delta_f = 15$ kHz
(M, N)	$(16, 8)$
Tap delays (ns)	$[0, 30, 150, 310, 370, 710, 1090, 1730, 2510]$
Tap powers (dB)	$-[0, 1.5, 1.4, 3.6, 0.6, 9.1, 7, 12, 16.9]$
Max. speed	500 km/h

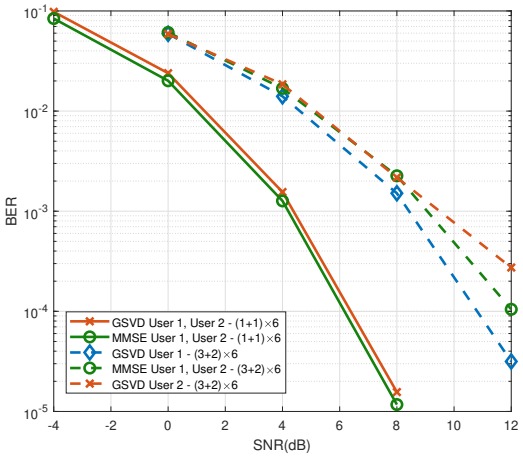

Figure 3: BER vs SNR uncoded scenario, comparing GSVD-based precoding and MMSE precoding.

As we will demonstrate later, this gap can be mitigated through the use of channel coding. In the $(3 + 2) \times 6$ configuration, the MMSE method achieves consistent performance for both users, while the GSVD approach shows improved performance for the first user compared to MMSE. However, for the second user, the GSVD approach performs similarly to MMSE, with a slight degradation at higher SNR values.

Fig. 4 presents the results for the same configurations but with LDPC coding applied. For the $(1 + 1) \times 6$ setup, the performance of GSVD matches that of MMSE, as predicted. In the $(3 + 2) \times 6$ configuration, the gap between the GSVD method for the second user and the MMSE method for both users is reduced. Additionally, the GSVD approach for the first user demonstrates better performance compared to MMSE.

In Fig. 5, the BER versus SNR for the coded case is plotted, considering an antenna configuration of $(3 + 2) \times 6$ in the presence of an estimation error. The channel coefficient in the time domain, h_k, is considered as a reference, while the estimated channel coefficient is expressed as $h_{k,\text{est}} = \rho h_k + \epsilon$ where ϵ is a Gaussian random variable of zero mean. In this formulation, ρ satisfies $0 \leq \rho \leq 1$, and the error term follows $E\{|\epsilon|^2\} = (1 - \rho^2)E\{|h_k|^2\}$. Here, $E\{\cdot\}$ represents the expected value. The analysis is conducted specifically for User 1. This figure demonstrates that the performance of GSVD is comparable to MMSE for the cases where $\rho = 0.99$ and $\rho = 0.995$, while exhibiting a slight improvement when $\rho = 0.999$.

5. CONCLUSION AND RESEARCH OPPORTUNITIES

In this study, we introduced the application of the GSVD technique within an uplink two-user MIMO-OTFS framework and provided analytical formulations for practical antenna configurations. The

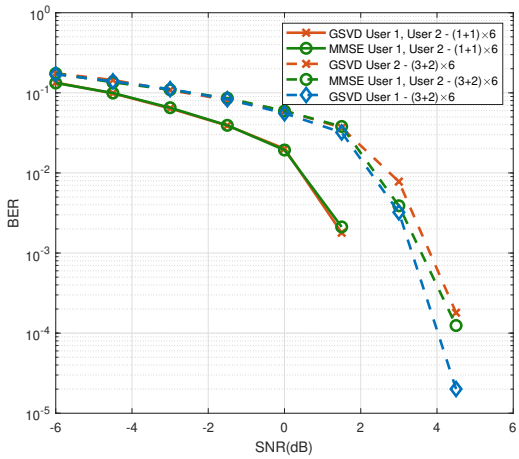

Figure 4: BER vs SNR for coded scenario, comparing GSVD-based precoding and MMSE equalization.

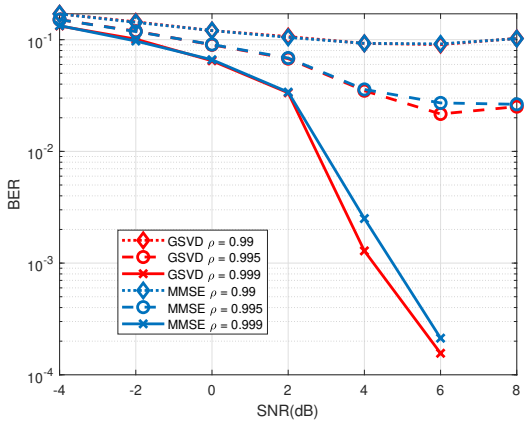

Figure 5: BER vs SNR for coded scenario in the presence of channel estimation error

methodology employs GSVD-based channel decomposition for each user, alongside the implementation of precoding and detection matrices. Simulation outcomes demonstrate that the proposed GSVD approach outperforms the conventional MMSE scheme under certain antenna configurations, while showing comparable results under others.

Exploring the extension of the GSVD approach to multi-user scenarios via HO-GSVD, for both uplink and downlink communication, represents a direction for future research.

Acknowledgement

This work was conducted within the MiFuture project, which has received funding from the European Union's Horizon Europe (HE) Marie Skłodowska-Curie Actions MiFuture HORIZON-MSCA2022-DN-01, under Grant Agreement number 101119643 and YAHYA/6G HORIZON-MSCA-2022-PF-01, under Grant Agreement number 101109435. It was partially supported by FCT/MECI through national funds and when applicable co-funded EU funds under UID/50008: Instituto de Telecomunicações.

Declaration on Generative AI

During the preparation of this work, the authors used CoPilot provided by Microsoft in order for editing and spell-checking the text.

References

[1] R. Hadani, S. Rakib, M. Tsatsanis, A. Monk, A. J. Goldsmith, A. F. Molisch, R. Calderbank, Orthogonal time frequency space modulation, in: 2017 IEEE Wireless Communications and Networking Conference (WCNC), 2017, pp. 1–6. doi:10.1109/WCNC.2017.7925924.

[2] P. Raviteja, K. T. Phan, Y. Hong, E. Viterbo, Interference cancellation and iterative detection for orthogonal time frequency space modulation, IEEE Transactions on Wireless Communications 17 (2018) 6501–6515. doi:10.1109/TWC.2018.2860011.

[3] Z. Wei, S. Li, W. Yuan, R. Schober, G. Caire, Orthogonal time frequency space modulation—part i: Fundamentals and challenges ahead, IEEE Communications Letters 27 (2023) 4–8. doi:10.1109/LCOMM.2022.3209689.

[4] S. Rakib, R. Hadani, Multiple access in wireless telecommunications system for high-mobility applications, 2017. US Patent.

[5] V. Khammammetti, S. K. Mohammed, Otfs-based multiple-access in high doppler and delay spread wireless channels, IEEE Wireless Communications Letters 8 (2019) 528–531. doi:10.1109/LWC.2018.2878740.

[6] B. V. S. Reddy, C. Velampalli, S. S. Das, Performance analysis of multi-user otfs, otsm, and single carrier in uplink, IEEE Transactions on Communications 72 (2024) 1428–1443. doi:10.1109/TCOMM.2023.3332865.

[7] B. V. Sudhakar Reddy, S. S. Das, C. Velampalli, G. S. Sanyal, Multi-user otfs with multi-antenna transmission, in: 2024 15th International Conference on Computing Communication and Networking Technologies (ICCCNT), 2024, pp. 1–7. doi:10.1109/ICCCNT61001.2024.10725940.

[8] A. Sattarzadeh, O. Dizdar, V. Battula, S. Wang, Low-complexity precoder design for mu-mimo otfs networks, IEEE Wireless Communications Letters (2025) 1–1. doi:10.1109/LWC.2025.3537293.

[9] S. Li, J. Yuan, P. Fitzpatrick, T. Sakurai, G. Caire, Delay-doppler domain tomlinson-harashima precoding for otfs-based downlink mu-mimo transmissions: Linear complexity implementation and scaling law analysis, IEEE Transactions on Communications 71 (2023) 2153–2169. doi:10.1109/TCOMM.2023.3244251.

[10] Y. Wang, Y. Zhang, Precoding design for uplink mu-mimo-otfs with statistical information of doppler shift, in: 2022 IEEE 22nd International Conference on Communication Technology (ICCT), 2022, pp. 157–161. doi:10.1109/ICCT56141.2022.10072599.

[11] Y. Hao, W. Shen, X. Bu, J. An, Precoding design for otfs-mimo system with beam squint effect, in: 2024 IEEE Wireless Communications and Networking Conference (WCNC), 2024, pp. 1–6. doi:10.1109/WCNC57260.2024.10570828.

[12] I. Umakoglu, M. Namdar, A. Basgumus, Deep learning-assisted signal detection for otfs-noma systems, IEEE Access 12 (2024) 119105–119115. doi:10.1109/ACCESS.2024.3449812.

[13] Z. Ding, Robust beamforming design for otfs-noma, IEEE Open Journal of the Communications Society 1 (2020) 33–40. doi:10.1109/OJCOMS.2019.2953574.

[14] S. Yang, H. Liu, Y. Zhou, Z. Ma, P. Fan, Joint precoding based on interference alignment and svd for mu-mimo otfs with mrc detector, IEEE Wireless Communications Letters 13 (2024) 2717–2721. doi:10.1109/LWC.2024.3442216.

[15] C. F. Van Loan, Generalizing the singular value decomposition, SIAM Journal on Numerical Analysis 13 (1976) 76–83.

[16] C. C. Paige, M. A. Saunders, Towards a generalized singular value decomposition, SIAM Journal on Numerical Analysis 18 (1981) 398–405.

[17] I. Kempf, P. J. Goulart, S. R. Duncan, A higher-order generalized singular value decomposition for rank-deficient matrices, SIAM Journal on Matrix Analysis and Applications 44 (2023) 1047–1072. URL: https://doi.org/10.1137/21M1443881. doi:10.1137/21M1443881. arXiv:https://doi.org/10.1137/21M1443881.

[18] D. Senaratne, C. Tellambura, Gsvd beamforming for two-user mimo downlink channel, IEEE Transactions on Vehicular Technology 62 (2013) 2596–2606. doi:10.1109/TVT.2013.2241091.

[19] Y. Hong, T. Thaj, E. Viterbo, Delay-Doppler Communications: Principles and Applications, Aca-

demic Press, 2022.

[20] ETSI (European Telecommunications Standards Institute), Evolved Universal Terrestrial Radio Access (E-UTRA); Base Station (BS) radio transmission and reception, Technical Report TS 136 104 V15.3.0, ETSI, 2018. URL: https://www.etsi.org/deliver/etsi_ts/136100_136199/136104/15.03.00_60/ts_136104v150300p.pdf.